New parametrization for spherically symmetric black holes in metric theories of gravity

Luciano Rezzolla[1,2] and Alexander Zhidenko[1,3]

[1]*Institut für Theoretische Physik, Goethe-Universität, Max-von-Laue-Str. 1, 60438 Frankfurt, Germany*
[2]*Max-Planck-Institut für Gravitationsphysik, Albert Einstein Institut, Am Mühlenberg 1, 14476 Potsdam, Germany*
[3]*Centro de Matemática, Computação e Cognição, Universidade Federal do ABC (UFABC), Rua Abolição, CEP: 09210-180, Santo André, SP, Brazil*

We propose a new parametric framework to describe in generic metric theories of gravity the spacetime of spherically symmetric and slowly rotating black holes. In contrast to similar approaches proposed so far, we do not use a Taylor expansion in powers of M/r, where M and r are the mass of the black hole and a generic radial coordinate, respectively. Rather, we use a continued-fraction expansion in terms of a compactified radial coordinate. This choice leads to superior convergence properties and allows us to approximate a number of known metric theories with a much smaller set of coefficients. The measure of these coefficients via observations of near-horizon processes can be used to effectively constrain and compare arbitrary metric theories of gravity. Although our attention is here focussed on spherically symmetric black holes, we also discuss how our approach could be extended to rotating black holes.

PACS numbers: 04.50.Kd,04.70.Bw,04.25.Nx,04.30.-w,04.80.Cc

arXiv:1407.3086v2 [gr-qc] 25 Sep 2014

I. INTRODUCTION

Black holes are one of the most intriguing, fascinating and yet unsettling consequences of classical general relativity. Even when putting aside the acceptance and understanding of the physical singularities hidden at their centers, the mere existence of an event horizon leads to a number of unsolved problems and long-standing debates. Yet, black holes are some of the most cherished objects in modern astronomy and evidence of their existence at different scales appears as common as it is convincing.

Proof of the existence of an event horizon would not be disputable if it appeared in terms of gravitational radiation, for instance in the form of a quasinormal mode ringdown when a new black hole is formed. However, it would become surely difficult, if possible at all, when using the electromagnetic emission coming from material accreting onto it [1]. At the same time, our increasing ability to perform astronomical observations that probe regions on scales that are comparable or even smaller than the size of the event horizon, will soon put us in the position of posing precise questions on the physical properties of those astronomical objects that appear to have all the properties of black holes in general relativity.

A good example in this respect is offered by astronomical observations of the radio compact source Sgr A*, which resides at the center of our Galaxy and is commonly assumed to be a supermassive black hole. Recent radio observations of Sgr A* have been made on scales comparable to what would be the size of the event horizon if it indeed were a black hole [2]. Furthermore, in the near future, very long baseline interferometric radio observations are expected to image the so-called black-hole "shadow" [3], namely the photon ring marking the surface where photons on circular orbits will have their smallest stable orbit [4]. These observations, besides providing the long-sought evidence for the existence of black holes, will also provide the possibility of testing the no-hair theorem in general relativity [5–7].

If sufficiently accurate, the planned astronomical observations will not only provide convincing evidence for the existence of an event horizon, but they will also indicate if deviations exist from the predictions of general relativity. However, given the already large number of alternative theories of gravity, and considering that this is only expected to grow in the near future, a case-by-case validation of a given theory using the observational data does not seem as viable an option. It is instead much more reasonable to develop a model-independent framework that parametrizes the most generic black-hole geometry through a finite number of adjustable quantities. These quantities must be chosen in such a way that they can be used to measure deviations from general relativity (or a black-hole geometry) and, at the same time, can be estimated robustly from the observational data [8].

This approach is not particularly new and actually similar in spirit to the parametrized post-Newtonian approach (PPN) developed in the 1970s to describe the dynamics of binary systems of compact stars [9]. A first step in this direction was done by Johannsen and Psaltis [10], who have proposed a general expression for the metric of a spinning non-Kerr black hole in which the deviations from general relativity are expressed in terms of a Taylor expansion in powers of M/r, where M and r are the mass of the black hole and a generic radial coordinate. While some of the first coefficients of the expansion can be easily constrained in terms of PPN-like parameters, an infinite number remains to be determined from observations near the event horizon [10]. This approach was recently generalized by relaxing the area-mass relation for non-Kerr black holes and introducing two independent modifications of the metric functions g_{tt} and g_{rr} [11]. Unfortunately, as discussed in [11], this approach can face some difficulties:

1. The proposed metric is described by an infinite number of parameters, which are roughly equally important in the strong-field regime, making it difficult to isolate the dominant terms.

2. The parametrization can be specialized to reproduce a spherically symmetric black hole metric in alternative theories only in the case in which the deviation from

the general relativity is small. This was checked for the black holes in dilatonic Einstein-Gauss-Bonnet gravity [12], for which the corresponding parameters were calculated only in the regime of small coupling.

3. At first order in the spin, the parametrization cannot reproduce deviations from the Kerr metric arising in alternative theories of gravity. As an example, it cannot reproduce the modifications arising for a slowly rotating black hole in Chern-Simons modified gravity.

In this paper we propose a solution to these issues and take another step in the direction of deriving a general parametrization for objects in metric theories of gravity. More precisely, we propose a parametrization for spherically symmetric and slowly rotating black hole geometries which can mimic black holes with a high accuracy and with a small number of free coefficients. This is achieved by expressing the deviations from general relativity in terms of a continued-fraction expansion via a compactified radial coordinate defined between the event horizon and spatial infinity. The superior convergence properties of this expansion effectively reduces to a few the number of coefficients necessary to approximate such spherically symmetric metric to the precision that can be in principle probed with near-future observations. While phenomenologically effective, the approach we suggest has also an obvious drawback. Because the metric expression we propose is not the consistent result of any alternative theory of gravity, it does not have any guarantee of being physically relevant or nothing more than a mathematical exercise.

The paper is organized as follows. In Sec. II we describe the proposed parametrization method. Sec. III is devoted to the relation between the proposed parameters and the parameters of the Johannsen-Psaltis spherically symmetric black hole. In Sec. IV we obtain values of the parameters that approximate a dilaton black hole, while in Sec. V we compare the photon circular orbit, the innermost stable circular orbit, and the quasinormal ringing predicted within our approximation with the corresponding quantities obtained for the exact solution of a dilaton black hole. In Sec. VI we apply our approach to slowly rotating black holes and, in the conclusions, we discuss applications for our framework and its possible generalization for the axisymmetric case. Finally, Appendix A is dedicated to a comparison of our parametrization framework with the alternative parametrization of a spherically symmetric black hole proposed in Ref. [11].

II. PARAMETRIZATION OF SPHERICALLY SYMMETRIC BLACK HOLES

The line element of any spherically symmetric stationary configuration in a spherical polar coordinate system (t, r, θ, ϕ) can be written as

$$ds^2 = -N^2(r)dt^2 + \frac{B^2(r)}{N^2(r)}dr^2 + r^2 d\Omega^2 \,, \tag{1}$$

where $d\Omega^2 \equiv d\theta^2 + \sin^2\theta d\phi^2$, and N and B are functions of the radial coordinate r only.

For any metric theory of gravity whose line element can be expressed as (1), we will next require that it could contain a spherically symmetric black hole[1]. By this we mean that the spacetime could contain a surface where the expansion of radially outgoing photons is zero, and define this surface as the event horizon. We mark its radial position as $r = r_0 > 0$ and this definition implies that

$$N(r_0) = 0 \,. \tag{2}$$

Furthermore, we will neglect any cosmological effect, so that the asymptotic properties of the line element (1) will be those of an asymptotically flat spacetime. Differently from previous approaches, we find it convenient to compactify the radial coordinate and introduce the dimensionless variable

$$x \equiv 1 - \frac{r_0}{r} \,, \tag{3}$$

so that $x = 0$ corresponds to the location of the event horizon, while $x = 1$ corresponds to spatial infinity. In addition, we rewrite the metric function N as

$$N^2 = xA(x) \,, \tag{4}$$

where

$$A(x) > 0 \quad \text{for} \quad 0 \leq x \leq 1 \,. \tag{5}$$

We further express the functions A and B after introducing three additional terms, ϵ, a_0, and b_0, so that

$$A(x) = 1 - \epsilon(1-x) + (a_0 - \epsilon)(1-x)^2 + \tilde{A}(x)(1-x)^3, \tag{6}$$

$$B(x) = 1 + b_0(1-x) + \tilde{B}(x)(1-x)^2, \tag{7}$$

where the functions $\tilde{A}$ and $\tilde{B}$ are introduced to describe the metric near the horizon (i.e., for $x \simeq 0$) and are finite there, as well as at spatial infinity (i.e., for $x \simeq 1$).

Since we are not considering any specific theory of gravity, we do not have precise constraints to impose on the metric functions N and B. At the same time, we can exploit the information deduced from the PPN expansion to constrain their asymptotic expression, i.e., their behaviour for $x \simeq 1$ [9]. More specifically, we can include the PPN asymptotic behaviour by expressing B and N as

$$\begin{aligned} N^2 &= 1 - \frac{2M}{r} + (\beta - \gamma)\frac{2M^2}{r^2} + \mathcal{O}\left(r^{-3}\right) \\ &= 1 - \frac{2M}{r_0}(1-x) + (\beta-\gamma)\frac{2M^2}{r_0^2}(1-x)^2 \\ &\quad + \mathcal{O}\left((1-x)^3\right) \,, \end{aligned} \tag{8}$$

$$\begin{aligned} \frac{B^2}{N^2} &= 1 + \gamma\frac{2M}{r} + \mathcal{O}\left(r^{-2}\right) = 1 + \gamma\frac{2M}{r_0}(1-x) \\ &\quad + \mathcal{O}\left((1-x)^2\right) \,. \end{aligned} \tag{9}$$

[1] Much of what discussed here for a black hole can be employed also for the spacetime of a compact star. In this case, however, suitable boundary conditions for the metric will need to be imposed at the stellar surface $x = 0$ [cf., Eq. (2)].

Here M is the Arnowitt-Deser-Misner (ADM) mass of the spacetime, while β and γ are the PPN parameters, which are observationally constrained to be [9]

$$|\beta-1| \lesssim 2.3\times 10^{-4}, \qquad |\gamma-1| \lesssim 2.3\times 10^{-5}\,. \tag{10}$$

Note that we have expanded the metric function g_{tt} to $\mathcal{O}\left((1-x)^3\right)$, but g_{rr} to $\mathcal{O}\left((1-x)^2\right)$. The reason for this difference is that the highest-order PPN constraint on g_{rr}, i.e., the parameter γ, is at first order in $(1-x)$. Conversely, the parameters β and γ set constraints on g_{tt} at second order in $(1-x)$.

By comparing the two asymptotic expansions (6)–(7) and (8)–(9), and collecting terms at the same order, we find that

$$1+\epsilon = \frac{2M}{r_0}\,, \tag{11}$$

$$a_0 = (\beta-\gamma)\frac{2M^2}{r_0^2}\,, \tag{12}$$

$$1+\epsilon+2b_0 = \gamma\frac{2M}{r_0}\,. \tag{13}$$

Hence, the introduced dimensionless constant ϵ is completely fixed by the horizon radius r_0 and the ADM mass M as

$$\epsilon = \frac{2M-r_0}{r_0} = -\left(1-\frac{2M}{r_0}\right)\,, \tag{14}$$

and thus measures the deviations of r_0 from $2M$. On the other hand, the coefficients a_0 and b_0 can be seen as combinations of the PPN parameters as

$$a_0 = \frac{(\beta-\gamma)(1+\epsilon)^2}{2}\,, \tag{15}$$

$$b_0 = \frac{(\gamma-1)(1+\epsilon)}{2}\,. \tag{16}$$

or, alternatively, as

$$\beta = 1+\frac{2\left[a_0+b_0(1+\epsilon)\right]}{(1+\epsilon)^2}\,, \tag{17}$$

$$\gamma = 1+\frac{2b_0}{1+\epsilon}\,. \tag{18}$$

Using now the observations constraints (10) on the PPN parameters, we conclude that a_0 and b_0 are both small and, in particular, $a_0 \sim b_0 \sim 10^{-4}$.

As mentioned above, the functions $\tilde{A}(x)$ and $\tilde{B}(x)$ have the delicate task of describing the black hole metric near its horizon and should therefore have superior convergence properties than those offered, for instance, by a simple Taylor expansion. We chose therefore to express them in terms of rational functions (see also Ref. [13]). Since the asymptotic behavior of the metric is fixed by the conditions (6)–(7), it is convenient to parametrize $\tilde{A}(x)$ and $\tilde{B}(x)$ by Padé approximants in the form of continued fractions, i.e., as

$$\tilde{A}(x) = \cfrac{a_1}{1+\cfrac{a_2 x}{1+\cfrac{a_3 x}{1+\ldots}}}\,, \tag{19a}$$

$$\tilde{B}(x) = \cfrac{b_1}{1+\cfrac{b_2 x}{1+\cfrac{b_3 x}{1+\ldots}}}\,, \tag{19b}$$

where $a_1, a_2, a_3 \ldots$ and $b_1, b_2, b_3 \ldots$ are dimensionless constants to be constrained, for instance, from observations of phenomena near the event horizon. A few properties of the expansions (19) are worth remarking. First, it should be noted that *at the horizon* only the first two terms of the expansions survive, i.e.,

$$\tilde{A}(0) = a_1\,, \qquad \tilde{B}(0) = b_1\,, \tag{20}$$

which in turn implies that near the horizon only the lowest-order terms in the expansions are important. Conversely, *at spatial infinity*

$$\tilde{A}(1) = \cfrac{a_1}{1+\cfrac{a_2}{1+\cfrac{a_3}{1+\ldots}}}\,, \qquad \tilde{B}(1) = \cfrac{b_1}{1+\cfrac{b_2}{1+\cfrac{b_3}{1+\ldots}}}\,. \tag{21}$$

Finally, while the expansions (19) effectively contain an infinite number of undetermined coefficients, we will necessarily consider only the first n terms. In this case, we simply need to set to zero the n-th terms, since if $a_n = 0 = b_n$, then all terms of order $m > n$ are not defined.

In practice, and as we will show in the rest of the paper, the superior convergence properties of the continued fractions (19) are such that the approximate metric they yield can reproduce all known (to us) spherically symmetric metrics to arbitrary accuracy and with a smaller set of coefficients. The inclusion of higher-order terms obviously improves the accuracy of the approximation but in general expansions truncated at $n = 4$ are more than sufficient to yield the accuracy that can be probed by present and near-future astronomical observations.

III. COMPARISON WITH THE JOHANNSEN-PSALTIS PARAMETRIZATION

To test the effectiveness of our approach in reproducing other known spherically symmetric metric theories of gravity, we obviously start from the Johannsen-Psaltis (JP) metric in the absence of rotation [10]. In this case, the black-hole line element is spherically symmetric and is given by the following expression for the slowly rotating dilaton black-hole

solution

$$ds^2 = -\left[1+h(r)\right]\left(1-\frac{2\tilde{M}}{r}\right)dt^2 + \left[1+h(r)\right]\left(1-\frac{2\tilde{M}}{r}\right)^{-1}dr^2 + r^2 d\Omega^2\,, \quad (22)$$

where the function h is a simple polynomial expansion in terms of the expansion parameter $\tilde{M}/r$, i.e.,

$$h(r) \equiv \sum_{n=1}^{\infty}\epsilon_n\left(\frac{\tilde{M}}{r}\right)^n = \epsilon_1\frac{\tilde{M}}{r} + \epsilon_2\frac{\tilde{M}^2}{r^2} + \epsilon_3\frac{\tilde{M}^3}{r^3} + \dots\,. \quad (23)$$

By construction, therefore, in the Johannsen-Psaltis metric the horizon is located at

$$r_0 = 2\tilde{M}\,, \quad (24)$$

while the relation between the ADM mass and the horizon mass $\tilde{M}$ is simply given by

$$M = \tilde{M}\left(1-\frac{\epsilon_1}{2}\right)\,. \quad (25)$$

We can now match the asymptotic expansions for the metrics (1) and (22). More specifically, we can compare Eqs. (6) and (23), to find that at $\mathcal{O}\left((1-x)^2\right)$ the following relations apply between our coefficients and those in the JP metric

$$\epsilon = -\frac{\epsilon_1}{2}\,, \quad (26a)$$

$$a_0 = -\frac{1}{2}\left(\epsilon_1 - \frac{\epsilon_2}{2}\right)\,. \quad (26b)$$

Similarly, comparing Eqs. (7) and (23), we find that at $\mathcal{O}\left(1-x\right)$

$$b_0 = \frac{\epsilon_1}{2}\,. \quad (26c)$$

It follows that if we set $\epsilon_1 = \epsilon_2 = 0$, as done originally in Ref. [10], then $\epsilon = 0 = a_0 = b_0$, thus implying that the PPN term are taken to be $\beta = \gamma = 1$. We will not make this assumption hereafter.

We can also match the expansions for the metrics (1) and (22) near the horizon. More specifically, we can obtain algebraic relations between our coefficients a_n, b_n and the coefficients ϵ_n of the JP metric by matching the g_{tt} and g_{rr} metric functions and their derivatives for $r \simeq r_0$ or $x \simeq 0$. A bit of tedious but straightforward algebra then leads to the following expressions

$$a_1 = h(r)\Big|_{\substack{r=r_0\\ \epsilon_1=\epsilon_2=0}} = \sum_{n=3}^{\infty}\frac{\epsilon_n}{2^n} = \frac{\epsilon_3}{8} + \frac{\epsilon_4}{16} + \frac{\epsilon_5}{32}\dots\,, \qquad b_1 = h(r)\Big|_{\substack{r=r_0\\ \epsilon_1=0}} = \sum_{n=2}^{\infty}\frac{\epsilon_n}{2^n} = \frac{\epsilon_2}{4} + \frac{\epsilon_3}{8} + \frac{\epsilon_4}{16} + \frac{\epsilon_5}{32}\dots\,, \quad (27a)$$

$$a_2 = -\frac{(r^3h)'}{r^2h}\Big|_{\substack{r=r_0\\ \epsilon_1=\epsilon_2=0}} = \frac{\sum_{n=4}^{\infty}\frac{\epsilon_n(n-3)}{2^n}}{\sum_{n=3}^{\infty}\frac{\epsilon_n}{2^n}}\,, \qquad b_2 = -\frac{(r^2h)'}{rh}\Big|_{\substack{r=r_0\\ \epsilon_1=0}} = \frac{\sum_{n=3}^{\infty}\frac{\epsilon_n(n-2)}{2^n}}{\sum_{n=2}^{\infty}\frac{\epsilon_n}{2^n}}\,, \quad (27b)$$

$$a_3 = \frac{h(r_0)^2r^3}{2a_1a_2}\left(\frac{(r^3h)'}{r^4h^2}\right)'\Big|_{\substack{r=r_0\\ \epsilon_1=\epsilon_2=0}}\,, \qquad b_3 = \frac{h(r_0)^2r^2}{2b_1b_2}\left(\frac{(r^2h)'}{r^2h^2}\right)'\Big|_{\substack{r=r_0\\ \epsilon_1=0}}\,, \quad (27c)$$

$$a_4 = \frac{1}{12a_1a_2a_3r^4}\left(r^2\left(r^2(r^3h)'\right)'\right)'\Big|_{\substack{r=r_0\\ \epsilon_1=\epsilon_2=0}} - \frac{(r^3h)'}{4a_1a_2a_3r^2}\left(\frac{\left(r^2(r^3h)'\right)'}{(r^3h)'}\right)'\Big|_{\substack{r=r_0\\ \epsilon_1=\epsilon_2=0}}\,, \quad (27d)$$

$$b_4 = \frac{1}{12b_1b_2b_3r^3}\left(r^2\left(r^2(r^2h)'\right)'\right)'\Big|_{\substack{r=r_0\\ \epsilon_1=0}} - \frac{(r^2h)'}{4a_1a_2a_3r}\left(\frac{\left(r^2(r^2h)'\right)'}{(r^2h)'}\right)'\Big|_{\substack{r=r_0\\ \epsilon_1=0}}\,, \quad (27e)$$

$$a_5 = \dots\,, \quad (27f)$$

where we have indicated with a prime $'$ the radial derivative.

Clearly, expressions (27) can be easily extended to higher or-

ders if necessary.

A few remarks are worth doing. First, because of cancellations, the terms $a_1, a_2, a_3 \ldots$ do not depend on ϵ_1 and ϵ_2; similarly, the terms $b_1, b_2, b_3 \ldots$ do not depend on ϵ_1, but they do depend on ϵ_2. Second, in the simplest case and the one considered in Ref. [10], i.e., when only $\epsilon_3 \neq 0$, the coefficient a_2 vanishes and our approximant for the function N reproduces it exactly. Finally, and more importantly, expressions (27) clearly show the rapid-convergence properties of the expansions (19). It is in fact remarkable that a few coefficients only are sufficient to capture the infinite series of coefficients needed instead in the JP approach [cf., for instance, expressions (27b) for the coefficients a_1 and b_1].

IV. PARAMETRIZATION FOR DILATON BLACK HOLES

As another test of the convergence properties of our metric parametrization we next consider a dilaton-axion black hole [14]. When both the axion field and the spin vanish, such a black hole is described by a spherically symmetric metric with line element

$$ds^2 = -\left(\frac{\rho-2\mu}{\rho+2b}\right)dt^2 + \left(\frac{\rho+2b}{\rho-2\mu}\right)d\rho^2 + (\rho^2+2b\rho)d\Omega^2\,. \tag{28}$$

The radial coordinate r and the ADM mass M are expressed, respectively, as

$$r^2 = \rho^2 + 2b\rho, \qquad M = \mu + b\,, \tag{29}$$

where b is the dilaton parameter.

By comparing now the expansions of (1) and (28) at spatial infinity, we find that

$$\epsilon = \sqrt{1+\frac{b}{\mu}} - 1\,, \tag{30a}$$

$$a_0 = \frac{b}{2\mu}\,, \tag{30b}$$

$$b_0 = 0\,, \tag{30c}$$

Similarly, by comparing the near-horizon expansions we find the other coefficients, which also depend on b/μ only and are given by

$$a_1 = 2\sqrt{1+\frac{b}{\mu}} + \frac{1}{1+b/(2\mu)} - 3 - \frac{b}{2\mu}\,, \tag{31a}$$

$$b_1 = \frac{\sqrt{1+b/\mu}}{1+b/(2\mu)} - 1\,, \tag{31b}$$

$$a_2 = \frac{\sqrt{1+\frac{b}{\mu}} - \frac{1}{2} - \frac{b^2}{4\mu^2} + \frac{b}{2\mu}\left(\sqrt{1+\frac{b}{\mu}}-1\right)}{\left(1+\frac{b}{2\mu}\right)^2}\,, \tag{31c}$$

$$b_2 = \frac{\sqrt{1+b/\mu}}{1+b/(2\mu)} - 1 - \frac{b^2}{(b+2\mu)^2}\,. \tag{31d}$$

It is clear that a_1 and b_1 vanish if $b = 0$, in which case we reproduce the line element of the Schwarzschild black hole exactly. If $b > 0$, on the other hand, we could in principle calculate as many coefficients of the continued fractions (19) as needed; in practice already the very first ones suffice. For example, for $b/\mu = 1$ and setting $a_3 = 0$, the maximum relative difference between the exact and the expanded expression for the metric function g_{tt} is $\lesssim 3\times 10^{-4}$. This relative difference becomes $\lesssim 3\times 10^{-6}$ if the order is increased of one, i.e., if $a_4 = 0$ (see also the discussion below on Fig. 1).

V. OBSERVABLE QUANTITIES WITHIN THE PARAMETRIZATION FRAMEWORK

A high precision in the mapping of the metric functions does not necessarily translate in an equivalent accurate measure of near-horizon phenomena. Hence, to further test the reliability of our continued-fraction expansions (19), we next compare a number of potentially observable quantities for a spherically symmetric dilaton black hole and for a black hole in Einstein-aether theory, respectively. More specifically, we calculate: the impact parameter for the photon circular orbit, the orbital frequency for the innermost stable circular orbit, and the quasinormal ringing of a massless scalar field. For all of these quantities, the metric is either expressed analytically [i.e., Eq. (28) for a dilation black hole] or numerically [i.e., for a black hole in Einstein-aether theory], or in its parametrized form [i.e., via the coefficients (30)–(31) for a dilation black hole].

A. Photon circular orbit and the innermost stable circular orbit

In a spherically symmetric spacetime, a photon circular orbit is defined as the null geodesic at radial position $r = r_{\rm ph}$ for which the following equations are satisfied

$$ds^2 = -N(r_{\rm ph})^2dt^2 + r_{\rm ph}^2 d\phi^2 = 0\,, \tag{32}$$

$$d^2 r_{\rm ph} = -\frac{N'(r_{\rm ph})N(r_{\rm ph})^3}{B(r_{\rm ph})^2}dt^2 + \frac{N(r_{\rm ph})^2 r_{\rm ph}}{B(r_{\rm ph})^2}d\phi^2 = 0\,, \tag{33}$$

where we have implicitly assumed $\theta = \pi/2$ because of the absence of a preferred direction. From these equations we find that the equation for the radius is given by

$$r_{\rm ph} = \frac{N(r_{\rm ph})}{N'(r_{\rm ph})}\,, \tag{34}$$

and that the corresponding orbital frequency $\Omega_{\rm ph}$ is

$$\Omega_{\rm ph} = \left.\frac{d\phi}{dt}\right|_{r=r_{\rm ph}} = \sqrt{\frac{N'(r_{\rm ph})N(r_{\rm ph})}{r_{\rm ph}}} = \frac{N(r_{\rm ph})}{r_{\rm ph}}\,. \tag{35}$$

Note that expression (35) depends only on the coefficients ϵ and a_n, but not on the b_n coefficients [cf., Eq. (4)]. We then

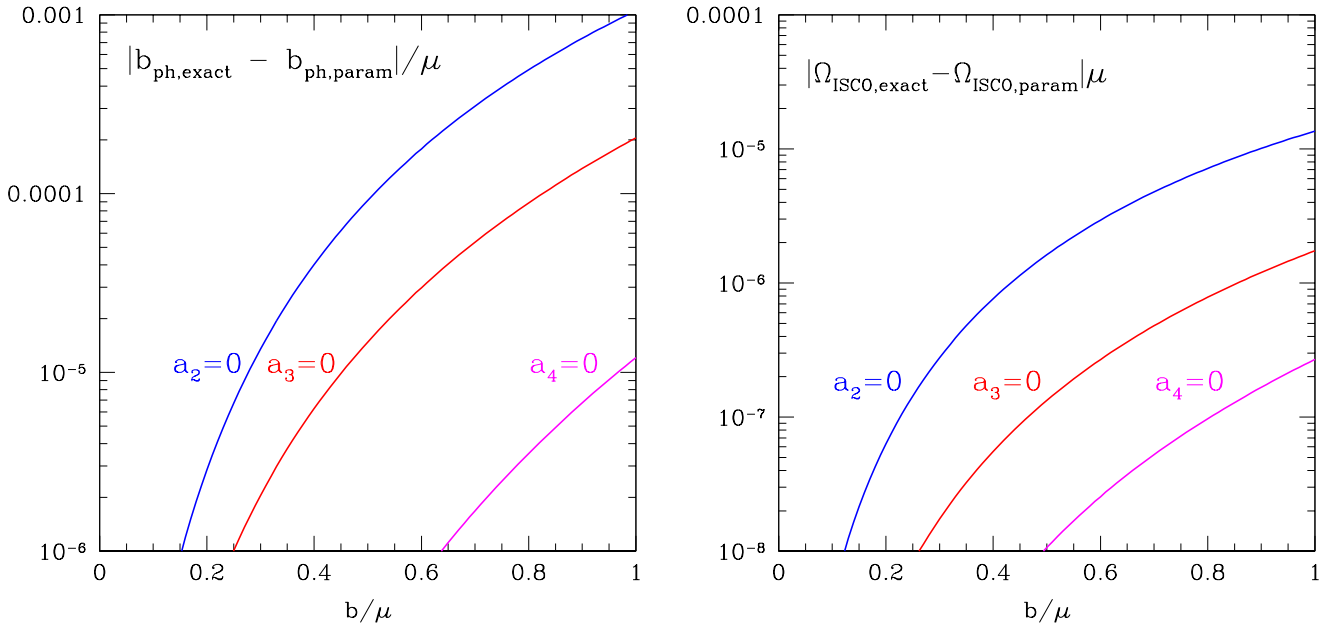

FIG. 1. *Left panel:* Difference between the exact values of the dilaton black hole orbit impact parameter for a circular orbit $b_{\rm ph}$ and the values obtained using the continued-fraction expansions (19). The results are shown as a function of the dimensionless strength of the dilaton parameter b/μ. Different lines refer to different levels of approximation, i.e., $a_2 = 0$ (blue line), $a_3 = 0$ (red line), and $a_4 = 0$ (magenta line). Note that even when $a_2 = 0$, the differences are $\lesssim 10^{-4}$ for $b \lesssim \frac{1}{2}\mu$. *Right panel:* The same as in the left panel but for the ISCO frequency.

define the impact parameter of the photon circular orbit (not to be confused with the dilaton parameter) as

$$b_{\rm ph} = \frac{1}{\Omega_{\rm ph}}\,. \tag{36}$$

whose analytic expression in the case of a dilaton black hole is [15]

$$b_{\rm ph} = \mu\sqrt{\frac{27 + 36b/\mu + 8b^2/\mu^2 + (9 + 8b/\mu)^{3/2}}{2}}\,, \tag{37}$$

which reduces to $b_{\rm ph}/\mu = 3\sqrt{3}$ in the case of a Schwarzschild black hole.

In the left panel of Fig. 1 we show the difference between the exact values of $b_{\rm ph}$ computed via Eq. (37) and the ones obtained after solving numerically Eq. (34) and making use the continued-fraction expansions (19) with coefficients (30)–(31). The differences are shown as a function of the dimensionless dilaton parameter b/μ and different lines refer to different levels of approximation, i.e., when setting $a_2 = 0$ (blue line), $a_3 = 0$ (red line), and $a_4 = 0$ (magenta line). The figure shows rather clearly that already when setting $a_2 = 0$, that is, when retaining only the coefficients ϵ, a_0, b_0, a_1, and b_1, the differences in the impact parameter are of the order of $\sim 10^{-4}\,\mu$ for $b \sim \frac{1}{2}\mu$. These differences become larger with larger dilaton parameter, but when $a_4 = 0$ they can nevertheless be reduced to be $\sim 10^{-6}\,\mu$ even for $b \sim \mu$.

In a similar way, we can calculate the innermost stable circular orbit (ISCO) exploiting the fact that the geodesic motion of a massive particle in the equatorial plane can be reduced to the one-dimensional motion within an effective potential

$$V_{\rm eff}(r) = \frac{E^2}{N^2(r)} - \frac{L^2}{r^2} - 1\,, \tag{38}$$

where E and L are the constants of motion, i.e., energy and angular momentum, respectively. A circular orbit then is the one satisfying the following conditions

$$V_{\rm eff}(r) = 0 = V'_{\rm eff}(r)\,. \tag{39}$$

while the ISCO is defined as the radial position r_o at which

$$V''_{\rm eff}(r_o) = 0\,. \tag{40}$$

Substituting (38) into (39) and (40), we obtain the following algebraic equation for the ISCO radius r_o,

$$3N(r_o)N'(r_o) - 3r_o N'^{\,2}(r_o) + r_o N(r_o)N''(r_o) = 0, \tag{41}$$

which we can solve numerically to calculate the corresponding orbital frequency as

$$\Omega_{\rm ISCO} = \sqrt{\frac{N'(r_o)N(r_o)}{r_o}}\,. \tag{42}$$

Here too, expression (42) depends only on the coefficients ϵ and a_n, but not on the b_n coefficients.

The ISCO frequency (42) can of course be compared with the exact expression in the case of a dilaton black hole, which is given by

$$\Omega_{\rm ISCO} = \frac{1}{2\mu}\sqrt{\frac{\kappa}{(1+\kappa)(1+\kappa+\kappa^2)^3}}\,, \tag{43}$$

where

$$\kappa \equiv \left(1+\frac{b}{\mu}\right)^{1/3}\,, \tag{44}$$

and expression (43) reduces to the well-known result of $\Omega_{\rm ISCO}\, M = (1/6)^{3/2}$ in the case of a Schwarzschild spacetime.

A comparison between the values of the ISCO frequency estimated from expressions (42) and (43) is shown in the right panel of Fig. 1, which reports the differences in units of μ and as a function of the dimensionless dilaton parameter b/μ. As for the left panel, different curves refer to different levels of approximation, i.e., $a_2 = 0$ (blue line), $a_3 = 0$ (red line), and $a_4 = 0$ (magenta line). Also in this case, the differences in the ISCO frequency are of the order of $\sim 10^{-6}\,\mu$ for $b \sim \frac{1}{2}\mu$ and can reduced to be $\sim 10^{-7}\,\mu$ even for $b \sim \mu$ by including higher-order coefficients.

Finally, we have compared the values for the impact parameter and the ISCO frequency also for another spherically symmetric black hole, namely, the one appearing in the alternative Einstein-aether theory of gravity [16]. In this case, the metric is not known analytically, but we have used the numerical data for the metric functions as discussed in Ref. [17]. More specifically, for a large number of pairs of the aether parameters c_+ and c_-, we have obtained a numerical approximation of the g_{tt} metric function $N(r)$ in terms of the coefficients ϵ, a_0, a_1, and a_2 of our continued-fraction expansions (19). Using these coefficients, we have then calculated numerically the values of $b_{\rm ph}$ and $\Omega_{\rm ISCO}$ as discussed above and compared with the corresponding values in general relativity.

The results of this comparison are reported in Fig. 2, whose left panel refers to the impact parameter for a circular photon orbit, while the right panel to the ISCO frequency. The two panels are meant to reproduce Figs. 2 and 4 of Ref. [17] and they do so with an accuracy of fractions of a percent. Note that the differences in $b_{\rm ph}$ and $\Omega_{\rm ISCO}$ with respect to general relativity can be quite large for certain regions of the space of parameters (e.g., $c_+ \simeq 1$). These regions, however, are de-facto excluded by the observational constraints set by binary pulsars (see the discussion in Ref. [18]).

B. Quasinormal ringing

Another way to probe whether the metric parametrization (1) and the continued fraction expansions (19) represent an effective way to reproduce strong-field observables near a black hole is to compare the response to perturbations. We recall, in fact, that if perturbed, a black hole will start oscillating. Such oscillations, commonly referred to as "quasinormal modes", represent exponentially damped oscillations that, at least at linear order, do not depend on the details of the source of perturbations, but only on the black hole parameters (see [19] for a review). The relevance of these oscillations is that they probe regions of the spacetime that are close to the light ring, but are global and hence do not depend on a single radial position. At the same time, the gravitational-wave signal from a perturbed black hole can be separated from a broad class of the environmental effects, allowing us to expect a good accuracy of the quasinormal modes' measurement [20]. Furthermore, both of the continued-fraction expansions (19) are involved and hence also some of the b_n coefficients will be nonzero.

For simplicity, we have considered the evolution of a massless scalar field Φ as governed by the Klein-Gordon equation

$$\Box\Phi = 0\,, \tag{45}$$

where $\Box$ is the Dalambertian operator. Substituting in (45) the ansatz

$$\Phi(t,r,\theta,\phi) = \Psi(t,r)Y_\ell(\theta,\phi)/r, \tag{46}$$

where $Y_\ell(\theta,\phi)$ are Laplace's spherical harmonics, we obtain for each multipole number ℓ the following wave-like equation,

$$\left(\frac{\partial^2}{\partial t^2} - \frac{\partial^2}{\partial r_*^2} + V_\ell(r)\right)\Psi(t,r) = 0\,, \tag{47}$$

where we have introduced the (tortoise-like) radial coordinate

$$dr_* = \frac{B(r)}{N^2(r)}dr\,, \tag{48}$$

and the effective potential is given by

$$V_\ell(r) = \frac{\ell(\ell+1)}{r^2}N^2(r) + \frac{1}{r}\frac{d}{dr_*}\frac{N^2(r)}{B(r)}\,. \tag{49}$$

It was shown in Ref. [13] that the rational approximation for $N(r)$ and $B(r)$ in some region near the black hole horizon in reduced Einstein-aether theory allows one to calculate accurately at least the quasinormal modes with the longest damping time. In order to test our approximation in the case of dilaton black hole, we have compared the black hole response in the time domain, found using either the exact representation of the metric (28) or the parametrized one via the coefficients (30)–(31).

The numerical solution of the evolution equation was made using a characteristic integration method that involves the light-cone variables $u \equiv t - r_*$ and $v \equiv t + r_*$ [21], with initial data specified on the two null surfaces $u = u_0$ and $v = v_0$. The results of these calculations are shown in Fig. 3, whose left panel reports the $\ell = 0$ solution of the scalar field at $r = 2r_0$ as function of time both in the case of an exact dilaton black hole (blue line) and of the corresponding parametrized expansion (red line). The relative differences are clearly very small already with $a_3 = 0 = b_3$, as shown in the right panel of Fig. 3, and amounting at most to fractions of a percent.

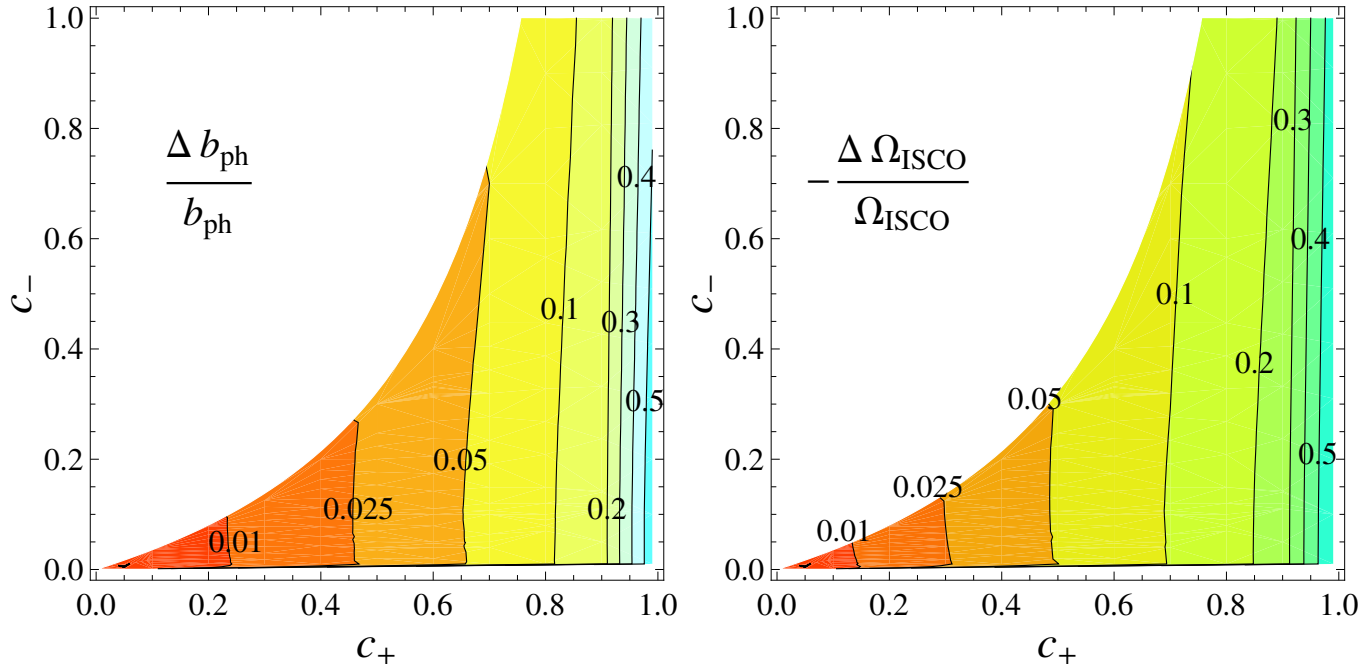

FIG. 2. *Left panel:* Relative difference in the photon circular orbit impact parameter $b_{\rm ph}$ between general relativity and the alternative Einstein-aether theory (cf., Fig. 4 of Ref. [17]). The differences are reported within the mathematically allowed ranges for the aether parameters c_+ and c_-. The contours correspond to the following values (from left to right): 0.01, 0.025, 0.05, 0.1, 0.2, 0.3, 0.4, 0.5. *Right panel:* the same as in the left panel but for the ISCO frequency (cf., Fig. 2 of Ref. [17]). The impact parameter and ISCO frequencies were calculated using continued-fraction expansions with $a_3 = 0$.

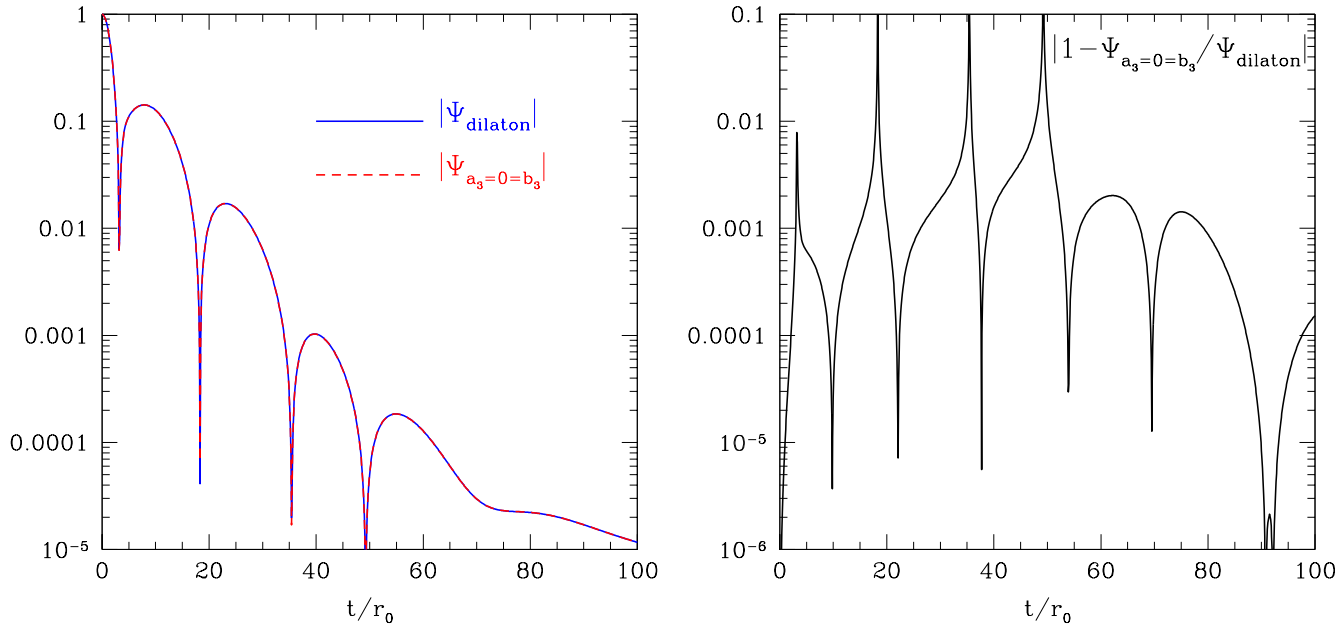

FIG. 3. *Left panel:* Evolution of the scattered scalar field $|\Psi|$ for the $\ell = 0$ perturbations at $r = 2r_0$ as computed using the exact dilaton black hole metric with $b/\mu = 1$ (blue solid line) or the corresponding parametrized form with $a_3 = 0 = b_3$ (red dashed line). *Right panel:* relative difference in the evolution of $|\Psi|$ shown in the left panel.

VI. SLOWLY ROTATING BLACK HOLES

We are in position now to make the first step towards the parametrization of black holes that are not spherically symmetric. We believe that the natural way to choose the parameters is taking into account the asymptotical behaviour of the corresponding metric, which is defined by multipole moments [22], as well as its near-horizon behaviour. Unfortunately, only a very limited number of such metrics is known in alternative theories of gravity that can be used for comparison. Indeed, to the best of our knowledge, a black hole with independent multipole moments was studied only in general relativity and discussed in Refs. [23, 24]. At the same time, even the parametrization of an axisymmetric stationary black hole is far from being a trivial question, since the corresponding metric is defined by four functions of two variables.

As a warm-up exercise, in this section we will consider spacetime metrics having only a small deviation from the spherical symmetry and hence extend the general expression (1) by introducing a new function ω in the $g_{t\phi}$ metric function and by retaining it only at the first order, i.e.,

$$\begin{aligned} ds^2 = &-N^2(r)dt^2 + \frac{B^2(r)}{N^2(r)}dr^2 + r^2 d\Omega^2 \\ &-2\omega(r,\theta) r^2 \sin^2\theta \, dt d\phi + \mathcal{O}(\omega^2)\,, \end{aligned} \tag{50}$$

and with the condition that ω has a falloff with radius that is faster than r^{-1}, i.e., that

$$r\omega(r,\theta) \ll 1\,, \tag{51}$$

implying that the event horizon remains at $r = r_0$ [2].

Because we are not considering any consistent (alternative) theory of gravity, but we are simply prescribing ad-hoc expression for the metric, we cannot impose additional constraints on the function ω. However, if we assume that the function ω depends on the radial coordinate r only, then we obtain a metric which can be associated with a slowly rotating black hole in Hořava-Lifshitz theory [25], in Einstein-aether gravity [26], in Chern-Simons modified gravity [27], or with dilatonic Einstein-Gauss-Bonnet [28] and dilaton-axion black holes [14].

In this case, the asymptotic behavior is given

$$\begin{aligned} \omega(r,\theta) \to \omega(r) &= \frac{2J}{r^3} + \mathcal{O}\left(r^{-4}\right) \\ &= \frac{2J}{r_0^3}(1-x)^3 + \mathcal{O}\left((1-x)^4\right)\,, \end{aligned} \tag{52}$$

where J is the spin of the black hole and we take it to be $J \ll M^2$.

The parametrization of the function ω can then be made in analogy with what was done for the nonrotating case and again we use a Padé approximation in terms of continued fractions in the form

$$\begin{aligned} r\omega(r) &= \left(\frac{r_0}{1-x}\right)\omega(x) \\ &= \omega_0(1-x)^2 + \cfrac{\omega_1(1-x)^3}{1+\cfrac{\omega_2 x}{1+\cfrac{\omega_3 x}{1+\ldots}}}\,. \end{aligned} \tag{53}$$

Since $r_0\omega(x) = \omega_0(1-x)^3 + \mathcal{O}\left((1-x)^4\right)$, the first coefficient is simply given by $\omega_0 \equiv 2J/r_0^2$, while the higher-order ones, $\omega_1, \omega_2, \omega_3 \ldots$, are fixed by comparing series expansion of ω near the event horizon r_0.

As an example, we consider the first-order correction to the dilaton black hole (28) due to rotation given by the following line element [14]

$$\begin{aligned} ds^2 = &-\left(\frac{\rho-2\mu}{\rho+2b}\right)dt^2 + \left(\frac{\rho+2b}{\rho-2\mu}\right)d\rho^2 \\ &-\left[\frac{4a(\mu+b)}{\rho+2b}\right]\sin^2\theta dt\, d\phi + (\rho^2+2b\rho)d\Omega^2 \\ &+\mathcal{O}(a^2). \end{aligned} \tag{54}$$

By comparing the asymptotical and near-horizon expansions we find that

$$\omega_0 = \frac{a}{2\mu}\,, \tag{55a}$$

$$\omega_1 = \frac{a}{2\mu}\left(\sqrt{\frac{\mu}{\mu+b}} - 1\right)\,, \tag{55b}$$

$$\omega_2 = \frac{\sqrt{\mu(\mu+b)} - \mu - b}{2\mu+b}\,, \tag{55c}$$

$$\omega_3 = \frac{\mu b}{(2\mu+b)^2}\,. \tag{55d}$$

Since we consider $a \ll \mu$, the coefficients (55) imply that $\omega_0 \ll 1$ and $\omega_1 \ll 1$, thus satisfying the constraint (51). The other coefficients are not small and depend on the dilaton parameter only. Of course, it is possible to find as many coefficients in (53) as needed for an accurate approximation for the function ω.

In order to test the convergence properties of (53) we again study the ISCO frequency for the equatorial orbits (i.e., $\theta = \pi/2$) of a massless particle in the background of a slowly rotating dilaton black-hole metric (50). In this case, the effective potential reads

$$V_{\rm eff}(r) = \frac{E^2 r^2 - 2EL\omega(r) r^2 - L^2 N^2(r)}{N(r)^2 r^2 + \omega(r)^2 r^4}\,. \tag{56}$$

We assume now that the energy E and the angular momentum L are positive, thus implying that $a > 0$ for the co-rotating and $a < 0$ for the counter-rotating particles, respectively. We then solve numerically the set of equations

$$V_{\rm eff}(r_o) = 0\,, \tag{57a}$$

$$V'_{\rm eff}(r_o) = 0\,, \tag{57b}$$

$$V''_{\rm eff}(r_o) = 0\,, \tag{57c}$$

[2] Determining in the metric (50) the location where $g^{rr} = 0$ will also involve the square of the metric function $g_{t\phi}$, which we take to be zero in the slow-rotation approximation.

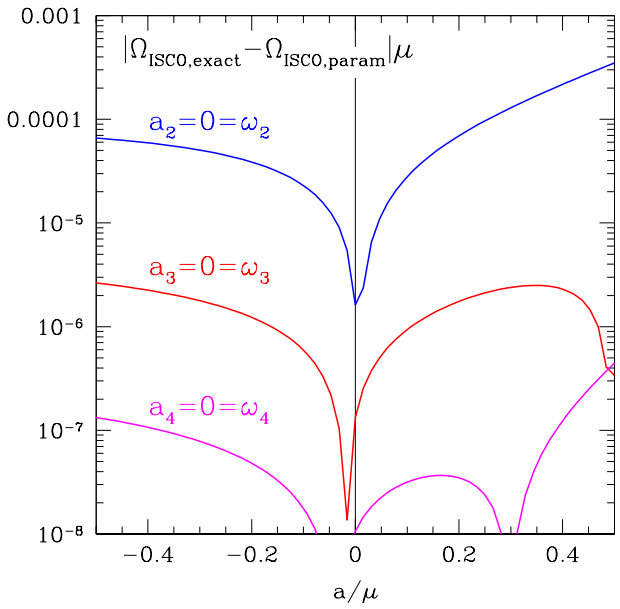

FIG. 4. Difference between the exact values of the ISCO frequencies in the equatorial plane for the dilaton black hole in the slow-rotation approximation regime and the values obtained using the continued-fraction expansions. Different curves, shown as functions of the rotation parameter, refer to the different levels of approximation: $a_2 = 0 = \omega_2$ (blue line), $a_3 = 0 = \omega_3$ (red line), and $a_4 = 0 = \omega_4$ (magenta line). In all cases we have taken a reference value of $b = \mu/2$.

finding at the radial coordinate of the ISCO $r_o > r_0$ the corresponding frequency $\Omega_{\rm ISCO}$

$$\Omega_{\rm ISCO} = \left.\frac{-g'_{t\phi} + \sqrt{{g'_{t\phi}}^2 - g'_{tt}g'_{\phi\phi}}}{g'_{\phi\phi}}\right|_{r=r_o} = \omega(r_o) + \frac{\omega'(r_o)r_o}{2} + \sqrt{\frac{N(r_o)N'(r_o)}{r_o} + \left(\omega(r_o) + \frac{\omega'(r_o)r_o}{2}\right)^2}\,. \quad (58)$$

Of course, these frequencies can be computed also for the parametrized metric (55) at different level of approximation. A comparison between the two calculations is summarized in Fig. 4, which shows the absolute value of the difference between the exact value of $\Omega_{\rm ISCO}$ and the approximate one as a function of the normalized spin parameter a/μ. As in the previous figures, here too different curves (all computed for $b = \mu/2$) refer to different degrees of approximation: $a_2 = 0 = \omega_2$ (blue line), $a_3 = 0 = \omega_3$ (red line), and $a_3 = 0 = \omega_3$ (magenta line). Also in this case it is apparent that the use of a larger number of coefficients in continued fraction expansions (19a) and (53), leads to a monotonic increase of the accuracy of the ISCO frequency.

As a concluding remark we note that a possible and rather popular approach to extend the parametrization (1) to rotating black holes would be the application of the Newman-Janis algorithm [29] to the metric (1) after having fixed the parameters $\epsilon, a_0, b_0, a_1, b_1, \ldots$. Although there is no proof that such a rotating configuration corresponds to a black hole solution in the same theory, the method works for some theories, e.g., the application of the Newman-Janis method to the metric (28) allows one to obtain the metric for the axion-dilaton black hole [30]. Therefore, it would be interesting to compare the coefficients (55) with those obtained at first order after the application of the Newman-Janis algorithm.

Yet, it is clear that this approach would not provide us with the most generic form for an axisymmetric black hole, simply because, in general, the geometry cannot be parametrized by one rotation parameter only. What is needed, instead, is a general framework which naturally comprises a set of parameters that account for the multipole moments of the spacetime and are not necessarily restricted to follow the relations expressed in terms of mass and angular momentum that apply for a Kerr black hole. Investigating this approach is beyond the scope of this initial paper, but will be the focus of our future work.

VII. CONCLUSIONS

We have proposed a new parametric framework to describe the spacetime of spherically symmetric and slowly rotating black holes in generic metric theories of gravity. The new framework provides therefore a link between astronomical observations of near-horizon physics with the properties of black holes in alternative theories of gravity, and which would predict deviations from general relativity. Unlike similar previous attempts in this direction, our approach is based on two novel choices. First, we use a continued-fraction expansion rather than the traditional Taylor expansion in powers of M/r, where M and r are respectively the mass of the black hole and a generic radial coordinate [10, 11]. Second, the expansion is made in terms of a compactified radial coordinate with values between zero and one between the horizon and spatial infinity. These choices lead to superior convergence properties and allows us to approximate a number of known metric theories with a much smaller set of coefficients.

These parameters can be calculated very accurately for any chosen spherically symmetric metric and, at the same time, they can be used via astronomical observations to measure near-horizon phenomena, such as photon orbits or the position ISCO. As a result, the new parametrization provides us with powerful tool to efficiently constrain the parameters of alternative theories using future astronomical observations.

Another important advantage of our approach is that we can use not only the asymptotic parameters from the PPN expansion, but also the near-horizon parameters, which are well-captured already by the first lowest-order coefficients. More specifically, the most important parameters for the near-horizon geometry are expressed simply in terms of the coefficients ϵ (which relates the ADM mass and the event horizon), a_1, b_1, and ω_1. The use of other higher-order parameters increases the accuracy of the approximation, but does not change significantly the observable quantities. The latter, in fact, are captured to the precision of typical near-future astronomical observations already at the lowest order.

The rapid convergence of our expansion is also useful for

the analysis of black-hole spacetimes in alternative theories where the metric is known only numerically. Using as a practical example the alternative Einstein-aether theory of gravity, we have shown that it is possible to reproduce to arbitrary accuracy the numerical results by using a small set of coefficients in the continued-fraction expansion. In turn, adopting such coefficients it is also possible to obtain an analytical representation of the metric functions, which can then be used to study the stability of such black holes, the motion of particles and fields in their vicinity [31], or to construct viable approximations for metrics with incorrect asymptotical behaviour, e.g., due to the presence of magnetic fields [32, 33].

As a concluding remark we note that our approach has so far investigated spherically symmetric spacetimes and hence black holes that are either nonrotating or slowly rotating. It would be interesting to find a generalization of our framework for the parametrization of axisymmetric black holes, for instance, via the application of the Newman-Janis algorithm. However, while this is technically possible, it is unclear whether such approach will turn out to be sufficiently robust. We believe, in fact, that a parametrization of axisymmetric black holes must combine, together with a rapidly converging expansion, also information on the parametrized post-Newtonian parameters, on the multipole moments, on the horizon shape, as well as parameters that define the near-horizon geometry. This task, which is further complicated by the lack of known axisymmetric back-hole solutions in alternative theories of gravity (cf., [34]), will be the focus of our future work.

Appendix A: Johannsen-Psaltis parametrization for the dilaton black hole

In order to explore convergence properties of our parametrization framework, we consider in this appendix the alternative parametrization of a spherically symmetric black hole in generic metric theories of gravity which has been recently proposed in Ref. [11],

$$ds^2 = -\left[1+h^t(r)\right]\left(1-\frac{2\tilde{M}}{r}\right)dt^2 + \left[1+h^r(r)\right]\left(1-\frac{2\tilde{M}}{r}\right)^{-1}dr^2 + r^2 d\Omega^2\,, \tag{A1}$$

where, instead of the function $h(r)$ in (22), two different functions are introduced:

$$h^t(r) \equiv \sum_{n=1}^{\infty}\epsilon_n^t\left(\frac{\tilde{M}}{r}\right)^n = \epsilon_1^t\frac{\tilde{M}}{r} + \epsilon_2^t\frac{\tilde{M}^2}{r^2} + \epsilon_3^t\frac{\tilde{M}^3}{r^3} + \dots\,, \tag{A2a}$$

$$h^r(r) \equiv \sum_{n=1}^{\infty}\epsilon_n^r\left(\frac{\tilde{M}}{r}\right)^n = \epsilon_1^r\frac{\tilde{M}}{r} + \epsilon_2^r\frac{\tilde{M}^2}{r^2} + \epsilon_3^r\frac{\tilde{M}^3}{r^3} + \dots\,. \tag{A2b}$$

In particular, we will determine the numerical values of the coefficients $\epsilon_1^t, \epsilon_1^r, \epsilon_2^t, \epsilon_2^r \dots$ to produce an approximation of the metric of a dilaton black hole (28). Although this can be done in different ways, the coefficients must obey the constraints that the theory naturally imposes on them. As a result, the large-distance properties of the functions $h^t(r)$ and $h^r(r)$ provide a series of constraints that fix the coefficients once an asymptotic expansion for the metric functions is made. In this way, we find that [cf., Eqs. (26) and (30)]

$$\tilde{M} = \sqrt{\mu(\mu+b)}, \tag{A3a}$$

$$\epsilon_1^t = 2 - 2\sqrt{1+\frac{b}{\mu}}, \tag{A3b}$$

$$\epsilon_2^t = \frac{2b}{\mu} + 4 - 4\sqrt{1+\frac{b}{\mu}}\,, \tag{A3c}$$

$$\epsilon_1^r = 0\,\dots\,. \tag{A3d}$$

Figure 5 shows the relative difference for the impact parameter of the photon circular relative to a dilaton black hole as computed using the parametrization (A2), and shown as function of the dimensionless strength of the dilaton parameter. Different lines refer to different levels of approximation, i.e., $0=\epsilon_4^t=\epsilon_5^t=\epsilon_6^t=\dots$ (blue line), $0=\epsilon_5^t=\epsilon_6^t=\epsilon_7^t=\dots$ (red line), and $0=\epsilon_6^t=\epsilon_7^t=\epsilon_8^t=\dots$ (magenta line), and so on. The dashed lines of the same color correspond to our continued-fraction approximation having the same number of parameters. More specifically, the first three of these lines should be compared with the corresponding ones in Fig. 1, in the following sense: considering, for instance, that the red line in Fig. 1 amounts to specifying four coefficients (i.e., ϵ, a_0, a_1, and a_2), which is the same number that is involved when considering the red line in Fig. 5 (i.e., ϵ_1^t, ϵ_2^t, ϵ_3^t, ϵ_4^t). Clearly, the errors in the novel parametrization are overall smaller for the same number of fixed coefficients in the expansion. A qualitatively similar figure can be produced also for the measurement of the ISCO but we do not report it here for compactness.

We should note that the errors in the parametrization (A2) can be made smaller if we fix the first two coefficients, i.e., ϵ_1^t and ϵ_2^t, from the asymptotic expansion at large distance, but we compute the remaining coefficients from the near-horizon behavior. This is simply because the impact parameter is a strong-field quantity and hence its approximation necessarily improves if the coefficients are constrained near the horizon. On the other hand, the real problematic feature of the parametrization (A2) is that the coefficients are roughly equally important near the horizon [11]. As a result, if one fixes the coefficients by matching the near-horizon behavior of the metric functions, the expression for the same coefficient will be different for different orders of approximations, making the approach not useful for constraining the parameters of the theory.

Finally, as mentioned in the Introduction, a particularly serious difficulty of the parametrization (A2) is that it does not reproduce the correct rotating metric even in the regime of slow rotation. This can be shown rather simply for the slowly rotating dilaton black hole, for which both the dilaton and the rotating Johannsen-Psaltis black hole can be obtained with the help of the Newman-Janis algorithm. More specifically, the

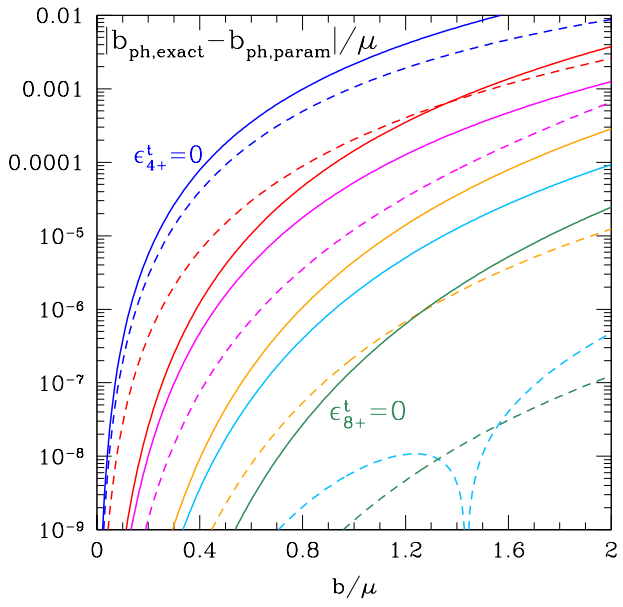

FIG. 5. Difference between the exact values of the dilaton black-hole orbit impact parameter for a circular orbit $b_{\rm ph}$ and the values obtained using the generalized Johannsen-Psaltis metric with the coefficients calculated by comparing the asymptotic expansions for the metric functions. The results are shown as a function of the dimensionless strength of the dilaton parameter b/μ. Different lines refer to different levels of approximation, i.e., $0 = \epsilon^t_4 = \epsilon^t_5 = \epsilon^t_6 = \ldots$ (blue line), $0 = \epsilon^t_5 = \epsilon^t_6 = \epsilon^t_7 = \ldots$ (red line), and $0 = \epsilon^t_6 = \epsilon^t_7 = \epsilon^t_8 = \ldots$ (magenta line), and so on. The dashed lines of the same color correspond to our continued-fraction approximation having the same number of parameters; hence the first three lines should be compared with those of Fig. 1 with the same color.

generalized Johannsen-Psaltis black hole in the regime of slow rotation reads [11]

$$\begin{aligned} ds^2 = &-\left[1+h^t(r)\right]\left(1-\frac{2\tilde{M}}{r}\right)dt^2 \\ &+\left[1+h^r(r)\right]\left(1-\frac{2\tilde{M}}{r}\right)^{-1}dr^2 + r^2 d\Omega^2 \\ &-2a\sin^2\theta\left(\sqrt{(1+h^t(r))(1+h^r(r))}\right. \\ &\left.-\left(1-\frac{2\tilde{M}}{r}\right)(1+h^t(r))\right)dt\,d\phi + \mathcal{O}(a^2). \end{aligned} \tag{A4}$$

By comparing the diagonal elements of (A4) and (54) we conclude that $r^2 = \rho^2 + 2b\rho$, while $h^t(r)$ and $h^r(r)$ must approximately be such that

$$\left(1-\frac{2\tilde{M}}{r}\right)(1+h^t) \simeq \frac{\rho-2\mu}{\rho+2b}\,, \tag{A5}$$

$$\sqrt{(1+h^t)(1+h^r)} \simeq \frac{d\rho}{dr} = \frac{r}{\rho+b} = \frac{\sqrt{\rho^2+2b\rho}}{\rho+b}\,. \tag{A6}$$

As a result, an inconsistency emerges for the off-diagonal element of the metric (A4), for which

$$\begin{aligned} \sqrt{(1+h^t)(1+h^r)} - &\left(1-\frac{2\tilde{M}}{r}\right)(1+h^t) \\ &\simeq \frac{\sqrt{\rho^2+2b\rho}}{\rho+b} - \frac{\rho-2\mu}{\rho+2b} \\ &\neq \frac{2(\mu+b)}{\rho+2b}\,, \end{aligned} \tag{A7}$$

unless $b \ll \rho$. Thus, for any approximation of the functions $h^t(r)$ and $h^r(r)$, the slowly rotating regime of the dilaton black hole is not reproduced by the metric (A4). Similar arguments were used to show that the Newman-Janis algorithm is not able to generate rotating black-hole solutions in modified gravity theories [35].

ACKNOWLEDGMENTS

It is a pleasure to thank E. Barausse for stimulating discussions and for providing us with the numerical data from [17]. We also thank E. Barausse, V. Cardoso, T. Johannsen, and D. Psaltis for useful comments and suggestions. A. Z. was supported by the Alexander von Humboldt Foundation, Germany, and Coordenação de Aperfeiçoamento de Pessoal de Nível Superior (CAPES), Brazil. Partial support comes from the DFG Grant No. SFB/Transregio 7 and by "NewCompStar", COST Action MP1304.

[1] M. A. Abramowicz, W. Kluzniak, and J. P Lasota, Astron. Astrophys. **396** L31-4 (2002)
[2] S. S. Doeleman *et al.*, Nature, **455**, 78 (2008).
[3] H. Falcke, F. Melia, and E. Agol, Astrophys. J. Lett., **528**, L13-16 (2000).
[4] T. Johannsen, D. Psaltis, S. Gillessen, D. P. Marrone, F. Ozel, S. S. Doeleman and V. L. Fish, Astrophys. J. **758**, 30 (2012) [arXiv:1201.0758 [astro-ph.GA]].
[5] C. Bambi and K. Freese, Phys. Rev. D **79**, 043002 (2009) [arXiv:0812.1328 [astro-ph]].
[6] T. Johannsen and D. Psaltis, Astrophys. J. **716**, 187 (2010) [arXiv:1003.3415 [astro-ph.HE]]; Astrophys. J. **718**, 446 (2010) [arXiv:1005.1931 [astro-ph.HE]].
[7] A. E. Broderick, T. Johannsen, A. Loeb and D. Psaltis,

arXiv:1311.5564 [astro-ph.HE].
[8] S. Vigeland, N. Yunes and L. Stein, Phys. Rev. D **83**, 104027 (2011) [arXiv:1102.3706 [gr-qc]].
[9] C. M. Will, Living Rev. Rel. **9**, 3 (2006) [gr-qc/0510072].
[10] T. Johannsen and D. Psaltis, Phys. Rev. D **83**, 124015 (2011) [arXiv:1105.3191 [gr-qc]].
[11] V. Cardoso, P. Pani and J. Rico, Phys. Rev. D **89**, 064007 (2014) [arXiv:1401.0528 [gr-qc]].
[12] P. Kanti, N. E. Mavromatos, J. Rizos, K. Tamvakis and E. Winstanley, Phys. Rev. D **54**, 5049 (1996) [hep-th/9511071]. P. Kanti, N. E. Mavromatos, J. Rizos, K. Tamvakis and E. Winstanley, Phys. Rev. D **57**, 6255 (1998) [hep-th/9703192].
[13] R. A. Konoplya and A. Zhidenko, Phys. Lett. B **644**, 186 (2007) [gr-qc/0605082]; Phys. Lett. B **648**, 236 (2007) [hep-th/0611226].
[14] A. Garcia, D. Galtsov and O. Kechkin, Phys. Rev. Lett. **74**, 1276 (1995).
[15] S. -W. Wei and Y. -X. Liu, JCAP **1311**, 063 (2013) [arXiv:1311.4251 [gr-qc]].
[16] T. Jacobson and D. Mattingly, Phys. Rev. D **64**, 024028 (2001) [gr-qc/0007031]; T. Jacobson, PoS QG **-PH**, 020 (2007) [arXiv:0801.1547 [gr-qc]].
[17] E. Barausse, T. Jacobson and T. P. Sotiriou, Phys. Rev. D **83**, 124043 (2011) [arXiv:1104.2889 [gr-qc]].
[18] K. Yagi, D. Blas, N. Yunes and E. Barausse, Phys. Rev. Lett. **112**, 161101 (2014) [arXiv:1307.6219 [gr-qc]]; Phys. Rev. D **89**, 084067 (2014) [arXiv:1311.7144 [gr-qc]].
[19] R. A. Konoplya and A. Zhidenko, Rev. Mod. Phys. **83**, 793 (2011) [arXiv:1102.4014 [gr-qc]].
[20] E. Barausse, V. Cardoso and P. Pani, Phys. Rev. D **89**, 104059 (2014) [arXiv:1404.7149 [gr-qc]].
[21] C. Gundlach, R. H. Price, and J. Pullin, Phys. Rev. D **49**, 883 (1994) [arXiv:gr-qc/9307009].
[22] F. D. Ryan, Phys. Rev. D **52**, 5707 (1995); Phys. Rev. D **55**, 6081 (1997); Phys. Rev. D **56**, 7732 (1997).
[23] N. A. Collins and S. A. Hughes, Phys. Rev. D **69**, 124022 (2004) [gr-qc/0402063].
[24] K. Glampedakis and S. Babak, Class. Quant. Grav. **23**, 4167 (2006) [gr-qc/0510057].
[25] E. Barausse and T. P. Sotiriou, Phys. Rev. D **87**, 087504 (2013) [arXiv:1212.1334]. A. Wang, Phys. Rev. Lett. **110**, 091101 (2013) [arXiv:1212.1876].
[26] E. Barausse and T. P. Sotiriou, Class. Quant. Grav. **30** (2013) 244010 [arXiv:1307.3359 [gr-qc]].
[27] K. Konno, T. Matsuyama and S. Tanda, Prog. Theor. Phys. **122**, 561 (2009) [arXiv:0902.4767 [gr-qc]]. N. Yunes and F. Pretorius, Phys. Rev. D **79**, 084043 (2009) [arXiv:0902.4669 [gr-qc]]; K. Yagi, N. Yunes and T. Tanaka, Phys. Rev. D **86**, 044037 (2012) [arXiv:1206.6130 [gr-qc]].
[28] P. Pani and V. Cardoso, Phys. Rev. D **79**, 084031 (2009) [arXiv:0902.1569 [gr-qc]]. P. Pani, C. F. B. Macedo, L. C. B. Crispino and V. Cardoso, Phys. Rev. D **84**, 087501 (2011) [arXiv:1109.3996 [gr-qc]]. D. Ayzenberg and N. Yunes, Phys. Rev. D **90**, 044066 (2014) [arXiv:1405.2133 [gr-qc]].
[29] E. T. Newman and A. I. Janis, J. Math. Phys. (N.Y.) **6**, 915 (1965); S. P. Drake and P. Szekeres, Gen. Relativ. Gravit. **32**, 445 (2000).
[30] S. Yazadjiev, Gen. Rel. Grav. **32**, 2345 (2000) [gr-qc/9907092].
[31] A. Zhidenko, arXiv:0705.2254 [gr-qc].
[32] R. A. Konoplya and R. D. B. Fontana, Phys. Lett. B **659**, 375 (2008) [arXiv:0707.1156 [hep-th]].
[33] K. D. Kokkotas, R. A. Konoplya and A. Zhidenko, Phys. Rev. D **83**, 024031 (2011) [arXiv:1011.1843 [gr-qc]].
[34] T. Johannsen, Phys. Rev. D **87**, no. 12, 124017 (2013) [arXiv:1304.7786 [gr-qc]].
[35] D. Hansen and N. Yunes, Phys. Rev. D **88**, no. 10, 104020 (2013) [arXiv:1308.6631 [gr-qc]].